Characterization of the effects involved in ultrasound-assisted extraction of trace elements from artichoke leaves and soybean seeds

Ignacio Machado, Ricardo Faccio, Mariela Pistón

PII: S1350-4177(19)30904-6
DOI: https://doi.org/10.1016/j.ultsonch.2019.104752
Reference: ULTSON 104752

To appear in: *Ultrasonics Sonochemistry*

Received Date: 19 June 2019
Revised Date: 24 July 2019
Accepted Date: 23 August 2019

Please cite this article as: I. Machado, R. Faccio, M. Pistón, Characterization of the effects involved in ultrasound-assisted extraction of trace elements from artichoke leaves and soybean seeds, *Ultrasonics Sonochemistry* (2019), doi: https://doi.org/10.1016/j.ultsonch.2019.104752

Characterization of the effects involved in ultrasound-assisted extraction of trace elements from artichoke leaves and soybean seeds

Ignacio Machado[a], Ricardo Faccio[b], Mariela Pistón[a*]

[a]*Grupo de Análisis de Elementos Traza y Desarrollo de Estrategias Simples para Preparación de Muestras (GATPREM), Analytical Chemistry, DEC, Faculty of Chemistry, Universidad de la República, Gral. Flores 2124, Montevideo, Uruguay*

[b]*Centro NanoMat, DETEMA, Faculty of Chemistry, Universidad de la República, Canelones, Uruguay*

*Corresponding author. E-mail: mpiston@fq.edu.uy

Abstract[1]

Ultrasonication is known to induce cavitation and can thus accelerate extraction, dissolution, digestion, and other processes, while the intense mixing caused by the propagation of ultrasound waves enhances analyte transfer to the extraction medium. Consequently, ultrasound-assisted extraction (UAE) is viewed as a simple procedure well suited for the extraction and subsequent determination of trace elements in food. Herein, we use different techniques to characterize several processes involved in probe- and bath-based UAE, apply them to the determination of trace metals (Cd, Cu, Ni, Pb, and Zn) in globe artichoke leaves and soybean seeds, and closely monitor the extraction rates of selected analytes. The developed UAE-based method is found to comply with the criteria of Green Chemistry and is concluded to be a reliable, simple, and cheap alternative to standard food analysis techniques.

Keywords: ultrasound-assisted extraction, trace elements, probe, bath, food

[1] Ultrasonication-assisted extraction, UAE; standard reference material, SRM; microwave-assisted acid digestion, MAE; scanning electron microscopy, SEM; Fourier transform infrared, FT-IR;

1. Introduction

One of the latest trends in analytical chemistry is the avoidance of harsh treatment during sample preparation and the search for efficient extraction procedures involving mild conditions to achieve shorter extraction times, reduced acid consumption, and energy/cost saving. Consequently, a number of enhanced and efficient extraction techniques have been established, e.g., ultrasound-assisted extraction (UAE), which allows rapid quantitative extractions of essential and potentially toxic trace elements from food samples to be carried out with high reproducibility. UAE-based methods are efficient alternatives to standard techniques for foodstuff and raw material analysis, allowing one to minimize the usage of concentrated mineral acids, simplify manipulation and work-up, and reduce the energy cost of extraction [1–4]. Despite these advantages, UAE-based methods of trace element determination in food have not yet been standardized.

When applied to homogeneous suspensions, ultrasonication can induce cavitation and thus accelerate extraction, dissolution, digestion, and other processes, additionally facilitating cell rupture (for biological samples) and the subsequent release of encapsulated analytes. Moreover, ultrasonication promotes the formation of oxidizing species and radicals ($OH^{\bullet}$ and H_2O_2) in liquid media, thus favoring the oxidation of organic matrices [3].

Among the various types of currently available instruments, ultrasonic baths and ultrasound probes are the ones most commonly used in analytical laboratories. Both of these instruments operate at a fixed frequency (usually 20 kHz for probes and 40 kHz for baths), with the cavitation efficiency of the probe exceeding that of the bath, as a higher

intensity is introduced to a specific area in the former case. Although the above equipment is less expensive than traditional microwave digestors used for the analysis of inorganic foodstuff constituents, as recommended by official methods, no hits related to “ultrasound” are returned if a search is performed in a seminal AOAC publication [5].

The effects of ultrasonication on certain properties such as emulsification capacity, solubility, and texture have been used to improve certain food technology processes and have also found applications in the fields of homogenization, viscosity change, extraction, drying, crystallization, and foam removal [6]. The thermal environment generated by cavitation leads to the occurrence of a variety of reactions including the generation of reactive radicals. Depending on the application, either the physical, chemical, or both effects of acoustic cavitation can be selectively used [7].

Although UAE-based methods of trace element determination in food samples have been widely investigated [4, 8–10], the origin of extraction efficiency enhancement has not been clearly identified. The implosion of cavitation bubbles on the matrix surface results in micro-jetting, which gives rise to phenomena such as surface peeling, erosion, and particle breakdown [2], while matrix fragmentation in liquid media during ultrasonication results in enhanced hydration and an increased analyte extraction index. Thus, UAE acts through different independent or combined mechanisms of fragmentation, erosion, capillarity, detexturation, and sonoporation [11].

The fragmentation phenomenon reported by several authors is related to the reduction of particle size during ultrasonication due to inter-particle collisions and shockwaves created by collapsing cavitation bubbles [12,13]. Notably, localized erosion is sometimes observed. The surface of vegetable tissues features different cellular structures (e.g., trichomes) that may be specifically impacted by ultrasound. Hence, theses structure may be

damaged or removed from the tissue after ultrasonication, which can be used for cleaning, sonochemical reactions, and other purposes [14].

Another effect of ultrasound is sonocapillarity, which refers to the increase of depth and velocity of liquid penetration into canals and pores under certain sonication conditions [15]. Although the corresponding mechanism is not fully understood, a relationship between cavitation and sonocapillarity has been established [16]. Finally, in some cases, UAE promotes the detexturation of plant structures and thus increases their accessibility to solvents [17].

Sonoporation, another common effect of ultrasound, can be used for reversible or irreversible cell membrane pore formation, which results in the release of cellular content into the extraction medium [2].

Although all of the above processes have been described as acting separately during UAE, a combination of their effects most probably occurs, e.g., the intense mixing due to the propagation of ultrasound waves in the liquid medium enhances mass transfer and thereby increases the analyte extraction rate [18].

Herein, we aimed to characterize some of the aforementioned processes by studying the extraction of trace metals (Cd, Cu, Ni, Pb, and Zn) from two different matrices, namely globe artichoke leaves (as a model of green vegetables) and soybean seeds (as a model of legumes). The discussion focused on the comparison of control samples extracted in the absence of ultrasound (only in acidic media) and those extracted by UAE in a dilute acidic medium using a bath and a probe. Extraction rates were monitored by atomic absorption spectrometry, and physical processes were examined by confocal Raman spectroscopy, scanning electron microscopy, and laser diffraction particle size analysis. In addition, a

validated green analytical method based on UAE was presented and confirmed to be a reliable alternative to standard methods.

2. Materials and methods

2.1. Reagents

Standard solutions for calibration curves were prepared by serial dilution of commercial stock solutions (1000 mg L^{-1}) of Cd, Cu, Ni, Pb, and Zn (Merck, Germany) in 0.1 mol L^{-1} HNO_3 prepared from concentrated HNO_3 (Merck, Germany). All other reagents were of analytical grade unless otherwise specified. Ultrapure water of 18.2 MΩ cm resistivity (ASTM Type I) was obtained using a Millipore™ DirectQ3 UV water purification system. All glassware was soaked overnight in 1.5 mol L^{-1} HNO_3 and then rinsed exhaustively with ultrapure water.

2.2. Samples

Globe artichoke leaves (*Cynara scolymus*) and soybean seeds (*Glycine max*) were collected in Montevideo, Uruguay, as described in previous works [1, 19]. Samples were washed with ultrapure water, dried in an oven with forced air circulation (70 °C), and stored at 20 °C.

Standard reference materials (SRMs) comprising wheat flour (NIST 1567b) and spinach leaves (NIST 1570a) were selected because of their similarities with the studied matrices and were used for trueness and precision evaluation after being subjected to the same treatment as the collected samples. The collected samples were dried and grounded using a blade mill and passed through a 200-µm sieve to achieve a particle size as close to

that of the corresponding SRM and obtain a homogeneous suspension, as particle size is a very important variable for increasing UAE efficiency.

2.3. Sample preparation procedures

2.3.1. Microwave-assisted digestion

The contents of Cd, Cu, Ni, Pb, and Zn were determined using microwave-assisted acid digestion (MAE) in a microwave oven (CEM™, Mars 6, 400–1800 W) equipped with 12 Easy Prep Plus™ vessels. Each vessel was charged with accurately weighed 0.5-g powdered samples and 10.0 mL of 3.5 mol L^{-1} HNO_3. For digestion, the power was varied between 400 and 1800 W, the temperature was increased to 200 °C in 15 min and held for 10 min, while the maximum pressure equaled 500 psi. The solution obtained after digestion was used for analytical determinations, which were carried out in triplicate. Reagent blanks were also run.

2.3.2. Probe-based UAE (UAE-probe)

Sample preparation was performed using an ultrasonic homogenizer (Sonics™ vibracell, 750 W; 20 kHz; 230 V_{AC}) equipped with a 13-mm Ti alloy probe. Typically, a 50-mL glass flask was charged with a 0.5-g sample and 10.0 mL of 3.5 mol L^{-1} HNO_3, and the probe was immersed into the resulting mixture for 10 min at 35% sonication amplitude. The obtained suspension was centrifuged for 3 min at 28,000 *g*, and the supernatant was used for analytical determinations, which were carried out in triplicate. Reagent blanks were also run.

2.3.3. Bath-based UAE (UAE-bath)

Samples were prepared using a Cole-Parmer™ 8893 ultrasonic bath (47 kHz; 230 V_{AC}). Typically, a 25-mL glass flask was charged with a 0.5-g sample and 10.0 mL of 3.5 mol L^{-1} HNO_3, and the vessel was put into the ultrasonic bath for 25 min. Up to 6 flasks were simultaneously introduced in the bath, previously, a verification of the highest point of cavitation was performed in order establish where to place de flasks. The obtained suspension was centrifuged for 3 min at 28,000 *g*, and the supernatant was used for analytical determinations, which were carried out in triplicate. Reagent blanks were also run. It is worth highlighting that up to six samples could be simultaneously treated in the 5-L bath.

2.4. Analytical determinations

Copper and zinc were quantified by flame atomic absorption atomic spectrometry using a Perkin Elmer™ AAnalyst 200 spectrometer (Norwalk, USA) operated at 324.75 nm (Cu) and 213.86 nm (Zn). Hollow cathode lamps from Photron™ (Narre Warren, Australia) were used. Flame composition was acetylene (2.5 L min^{-1}) and air (10.0 L min^{-1}).

Cadmium, nickel, and lead were quantified by electrothermal atomic absorption spectrometry (Thermo Scientific™ iCE 3500 spectrometer, Cambridge, United Kingdom) employing Zeeman correction, as the levels of the above analytes were low. A transversely heated graphite tube furnace module from Thermo Fisher Scientific™ was used. Analytical lines at 228.8 nm (Cd), 232.0 nm (Ni), and 283.3 nm (Pb) were employed, and integrated absorbance was used for quantitation. Pyrolytically coated graphite tubes from Thermo Scientific were employed, and, except for the atomization step, Ar (99.998%, Air Liquide, Uruguay) was used as the purge and protective gas at a flow rate of 0.2 mL min^{-1}. The

injection volume equaled 30 μL. The chemical matrix modifiers for Cd and Pb were $Pd(NO_3)_2$ (5 μg) and $NH_4H_2PO_4$ (50 μg) respectively. No modifier was used for Ni. Optimized pyrolysis and atomization temperatures were 800 and 1800 °C (Cd), 1000 and 2500 °C (Ni), and 900 and 1400 °C (Pb), respectively.

2.5. Confocal Raman spectroscopy measurements

Physical and structural phenomena were examined by confocal Raman microscopy using a WITec Alpha™ 300-RA Raman confocal microscope. A small amount of the sample (control and solid residue) was deposited on glass to proceed with optical and Raman imaging in air. Raman spectra were collected using a laser with an excitation wavelength of 785 nm. The power of the excitation laser was adjusted between 10 and 20 mW to avoid sample damage. A set of 100 spectra (acquisition time = 0.2 s each) was averaged for each sample.

2.6. Particle size analysis by laser diffraction

The particle size distributions of control samples and sonicated suspensions were measured with a Coulter™ LS230 laser diffraction analyzer. The instrument routinely measured the particle size distributions (0.04–2000 μm) of residues obtained after procedures 2.3.2 and 2.3.3 using the diffraction of 750-nm laser light into 126 photodiode detectors. This rapid and non-destructive technique featured a sample turnaround time of 3–4 min. The basic operating procedure required samples to be disaggregated and dispersed in distilled water to form a slurry prior to introduction into the fluid module. The instrument was operated via a PC running specialized “Particle Characterization” software under the Microsoft Windows™ operating system. A Fraunhofer mathematical model was used by

default to calculate particle size based on the concentric ring pattern of light-scatter from the laser beam. The amount of sample required was determined by the obscuration percentage of the laser beam passing through the sample cell, with the recommended range lying between 8 and 12%.

2.7. Scanning electron microscopy (SEM)

SEM analysis was performed using a Jeol JSM-5900LV™ (USA) microscope. Samples (control and solid residue) required pre-fixation and were covered with an ultrathin Au layer (to conduct away the accumulated surface electrostatic charge) using a Denton Vacuum Desk II (USA) sputter coater.

Images were acquired in low vacuum (0.80 Torr) at an operating voltage of 15 kV, a probe current of 0.3 nA, and a working distance of 10 mm. Randomly selected areas were imaged at high resolution for each sample, and the dimension of each area was selected to be sufficiently representative of the whole sample. For a more accurate analysis of fine residues, SEM images were acquired at a high resolution of ~45 nm per pixel.

2.8. Fourier transform infrared spectroscopy (FT-IR)

FT-IR spectra (Shimadzu IR Prestige21) were recorded for samples pelletized with KBr in transmission mode and a frequency range of 400–4000 cm^{-1} with a resolution of 4 cm^{-1} using 20 scans and the Happ-Genzel apodization function. Data analysis was performed using IR Solution™ software.

3. Results and discussion

3.1. MAE vs. UAE

Total samples digestions were performed by means of MAE. The method was validated for Cd, Cu, Ni, Pb, and Zn determinations in selected matrices based on the recommendations of the Eurachem Guide, with the main figures of merit selected as explained in previous works [1,19,20]. For trueness evaluation, a Student's *t*-test–based comparative study was performed to probe the difference between the obtained values and determine the certified values of the analyzed SRM. At the 95% confidence level, the concentrations did not significantly differ from certified values. Precision (repeatability) expressed as RSD (%) for SRM analysis (n = 6) was better than 10% for all elements. Thus, the method was sufficiently accurate. The detection limits of Cd, Cu, Ni, Pb, and Zn (expressed as 3σ, n = 10, dry basis) were 0.002, 0.160, 0.020, 0.012, and 0.090 mg kg^{-1}, respectively.

The results obtained for both matrices are presented in Table 1. Since MAE is widely used for trace element determination in food, and prior validation confirmed its reliability, the values obtained using this procedure were considered as references for real samples. The results were compared with those obtained using the newly developed probe- and bath-based UAE methods and were found to be equivalent to the latter for all analytes. Therefore, the proposed methods were concluded to be adequate for the analysis of the studied elements in these matrices.

Although both bath- and probe-based methods yielded equivalent results, it is worth mentioning that an ultrasonic bath allows several samples to be treated simultaneously, with the exact number of samples depending on bath capacity. In this work, six samples were simultaneously sonicated with good reproducibility. In the case of the probe, only one

sample can be treated at a time, which increases the analysis time and poses the risk of cross contamination, as the probe must be submerged into the suspension.

3.2. Effects of ultrasound on vegetal matrices

3.2.1. Fragmentation

The impact of ultrasonication-induced fragmentation was illustrated through the example of Cu extraction from artichoke leaves and soybean seeds (Fig. 1) using the 20-kHz ultrasound probe and the 47-kHz ultrasound bath. Notably, quick fragmentation of leaves was observed during the first minutes of probe-based sonication, whereas this effect was less pronounced when the bath was used. The kinetics of Cu extraction was monitored by atomic absorption spectrometry (Figs. 1a and 1c), and a linear Cu concentration increase with time was initially observed for probe-based UAE, which corresponded to a direct solubilization of Cu. This effect was ascribed to the quicker reduction of particle size caused by the more intimate contact with the probe. In fact, quantitative extraction was achieved between 8 and 10 min in the case of UAE-probe, whereas a longer time of 18–25 min was required for UAE-bath.

UAE-probe artichoke residues were collected after filtration to measure the particle size distribution (Fig. 1b), and the average particle size after 20-min UAE-probe was determined as 160 µm, which was lower than that of the control (200 µm). However, no significant changes in the average particle size occurred between 10 and 20 min of sonication time, in agreement with the rapid fragmentation observed within the first 10 min.

A similar phenomenon was also observed for Cu extraction from soybean seeds, i.e., quick seed fragmentation occurred during the first minutes of probe-based sonication.

Quantitative extraction was achieved after 8 min in the case of UAE-probe and after 18 min in the case of UAE-bath (Fig 1c). UAE-probe soybean residues were collected after filtration to measure the particle size distribution (Fig. 1d). The particle size remarkably decreased with increasing sonication time, changing from 200 µm in the control sample to 80 µm after 10-min sonication and to 10 µm after 20-min sonication. Although fragmentation was observed for both vegetable matrixes, it was much more pronounced in the case of soybean seeds, leading to an almost complete solubilization after 30-min sonication. As previously stated, this phenomenon was ascribed to inter-particle collisions and shockwaves created by collapsing cavitation bubbles in the liquid. A direct consequence of this particle size reduction is the increase of the surface area of the solid, and, hence, more pronounced mass transfer and increased extraction rate and yield.

This physical effect of UAE was also studied by FT-IR and Raman spectroscopy, which are versatile and powerful analytical techniques that can be applied to microanalysis, provide optimal visual inspection, and feature chemical imaging and mapping. The selectivity for functional groups is different for each technique, and together they can provide complementary information, allowing one to better elucidate the sample structure [21]. Optical images shown in Fig. 2 were used to establish differences in the sample surface between the control soybean sample and residues obtained after 10-min sonication using the bath or the probe. Differences between the control soybean sample and the UAE-bath residue were negligible, whereas the UAE-probe residue featured a smoother surface than that of the control sample, which was attributed to the stronger impact of the probe caused by its higher sonication intensity and intimate contact.

Figure 2d presents the Raman spectra of the control soybean sample and the residues obtained after probe-based sonication. The control spectra featured an important

fluorescence contribution that was partially removed after baseline correction. The band centered at 1038 cm^{-1} (NO_3^-) was the only one that gained intensity after sonication, which was ascribed to the dissociation of residual HNO_3 in the dry sample [22]. Comparison of the three spectra allowed us to observe how the matrix surface changed with increasing sonication time. This effect was monitored as a reduction in the fluorescence contribution that improved the definition of vibrational bands.

The intensity of some Raman bands decreased after 20-min sonication, probably because of the lysis of cell walls and the partial decomposition of constituent organic matter. Concomitantly, characteristic bands associated with the O=CNH amide group appeared, namely signals associated with coupled C–N stretching and N–H bending vibrations and located at 1480–1580 cm^{-1} (amide II) and 1230–1300 cm^{-1} (amide III). At this point, it is worth mentioning that the wavenumber of amide modes reflects the structure of the main polypeptide chain irrespective of side groups [23]. The observed Raman bands and their proposed assignments are listed in Table 2.

The insights gained from Raman spectra were complemented with the information obtained from FT-IR spectra (Fig. 3). The IR bands associated with proteins were located at 1340–1380 cm^{-1} (amide III), 1520–1570 cm^{-1} (amide II, C–N stretching and N–H bending), and 1620–1680 cm^{-1} (amide I) [24]. Amide I and amide III signals seemed to be specifically impacted by sonication (especially the former), in accordance with the fact that peptides are degraded by ultrasound energy. The N–H stretching vibration at 3090–3700 cm^{-1} also seemed to be impacted, which was also indicative of protein modification.

3.2.2. Erosion

SEM imaging of artichoke leaf surface before and after UAE-probe showed localized erosion. Specifically, the glandular trichomes and covering hairs on artichoke leaves [25] seemed to be specifically impacted by ultrasound (Fig. 4). Hence, these structures were damaged or removed from the leaf after ultrasonication. Erosion enhanced the accessibility of diluted acid to leaves, improving extraction and solubilization rates. Given these observations, we hypothesized that the implosion of cavitation bubbles on the leaf surface induces the erosion of plant structures released in the extraction medium (Fig. 4c), as has previously been observed for boldo leaves [26].

A similar effect was observed for soybean seeds (Fig. 5), in which case rounded structures were impacted by ultrasound energy, and the surface therefore became remarkably smoother with increasing sonication time.

3.2.3. Detexturation

After a certain sonication time, a destruction or detexturation of plant structures was observed, e.g., distinguishable physical modifications of soybean seeds were noticed. Untreated seeds appeared filled and intact, while observations of seed residues after UAE-probe allowed us to identify different modifications (Fig. 6). After 25 min, gradual tissue degradation was observed, and after 30 min, cell structures were mostly broken and converted to undefined shapes (Fig. 6c). It was assumed that such cell disruption favored accessibility to the solvent. This detexturation of cell structures after UAE has rarely been reported, but some works indicate its destructive effect on cellular tissues, as described by Chemat *et al.* in a study of essential oil extraction from caraway seeds [27].

3.3. Combination of mechanisms

The UAE of trace elements from vegetal matrixes has been shown to involve fragmentation, erosion, and detexturation, with evidence of each effect provided separately. However, these processes most likely act in combination, probably in a sequential way. Moreover, the transfer of analytes to the liquid medium is enhanced by the intense mixing caused by the propagation of ultrasound waves. The combination of all these physical impacts leads to the high efficiency of UAE. Additionally, the type of sample and applied pretreatments (milling and sieving) have a major impact on the extraction index.

Even though the examples shown in Fig. 1 are related to Cu extraction, the corresponding phenomena are also involved in the release of other trace elements from the same matrices. As a matter of fact, the UAE-probe procedure described in Section 2.3.2 (with a 10 min sonication time) and the UAE-bath procedure described in Section 2.3.3 (with a 25 min sonication time) were suitable for the quantitation of Cd, Cu, Ni, Pb, and Zn, as shown in Table 1. The difference in optimum sonication time between bath- and probe-based extractions is reasonable, since the increased power output of ultrasonic probes provides more energy in the sinus of the suspension and increases the temperature of the medium, e.g., the final temperature of our suspension reached 80 °C when the probe was used.

4. Conclusions

Bath- and probe-based UAE methods were developed for the determination of Cd, Cu, Ni, Pb, and Zn in globe artichoke leaves and soybean seeds. The phenomena involved in the UAE were studied and discussed in detail. Although these phenomena were studied separately, they probably act in combination (sequentially) during the extraction process. The intense mixing caused by the propagation of ultrasound waves also enhances analyte

transfer to the acid medium. Therefore, this work contributes to a better understanding of the successful use of UAE for foodstuff analysis.

Even though the optimum sonication time for UAE-probe was almost half of that of UAE-bath, this disadvantage can be viewed as negligible, as the bath allows several samples to be treated at the same time with a minimum risk of cross contamination.

Both methods feature the use of dilute nitric acid and do not require external heating, in good agreement with the principles of green chemistry, and can therefore be proposed as simple and economical alternatives to existing techniques.

Disclosure statement

The authors declare that there is no conflict of interest regarding the publication of this article.

Acknowledgements

The authors thank Agencia Nacional de Investigación e Innovación (ANII), Comisión Sectorial de Investigación Científica (CSIC), and PEDECIBA-Química.

References

[1] I. Machado, I. Dol, E. Rodríguez-Arce, M.V. Cesio, M. Pistón, Comparison of different sample treatments for the determination of As, Cd, Cu, Ni, Pb and Zn in globe artichoke (*Cynara cardunculus* L. subsp. Cardunculus), Microchem. J. 128 (2016) 128–133. https://doi.org/10.1016/j.microc.2016.04.016

[2] F. Chemat, N. Rombaut, A.G. Sicaire, A. Meullemiestre, A.S. Fabiano-Tixier, M. Abert-Vian, Ultrasound assisted extraction of food and natural products. Mechanisms,

techniques, combinations, protocols and applications. A review, Ultrason. Sonochem. 34 (2017) 540–560. https://doi.org/10.1016/j.ultsonch.2016.06.035

[3] C. Bendicho, I. De La Calle, F. Pena, M. Costas, N. Cabaleiro, I. Lavilla, Ultrasound-assisted pretreatment of solid samples in the context of green analytical chemistry, Trends Anal. Chem. 31 (2012) 50–60. https://doi.org/10.1016/j.trac.2011.06.018

[4] S. Seidi, Y. Yamini, Analytical sonochemistry; developments, applications, and hyphenations of ultrasound in sample preparation and analytical techniques, Cent. Eur. J. Chem. 10 (2012) 938–976. https://doi.org/10.2478/s11532-011-0160-1

[5] G.W. Latimer, Jr. (Ed), Official Methods of Analysis of AOAC International, 20th ed., Rockville, MA, 2016.

[6] A.C. Soria, M. Villamiel, Effect of ultrasound on the technological properties and bioactivity of food: a review, Trends Food Sci. Technol. 21 (2010) 323–331.

[7] M. Ashokkumar, Applications of ultrasound in food and bioprocessing, Ultrason. Sonochem. 25 (2015) 17–23. https://doi.org/10.1016/j.tifs.2010.04.003

[8] H. Ebrahimi-Najafabadi, A. Pasdaran, R. Rezaei Bezenjani, E.A. Bozorgzadeh, Determination of toxic heavy metals in rice samples using ultrasound assisted emulsification microextraction combined with inductively coupled plasma optical emission spectroscopy, Food Chem. 289 (2019) 26–32. https://doi.org/10.1016/j.foodchem.2019.03.046

[9] N. Altunay, A. Elik, C. Bulutlu, R. Gürkan, Application of simple, fast and eco-friendly ultrasound-assisted-cloud point extraction for pre-concentration of zinc, nickel and cobalt from foods and vegetables prior to their flame atomic absorption spectrometric determinations, Int. J. Environ. Anal. Chem. 98 (2018) 655–675. https://doi.org/10.1080/03067319.2018.1487063

[10] I. Machado, G. Bergmann, M. Pistón, A simple and fast ultrasound-assisted extraction procedure for Fe and Zn determination in milk-based infant formulas using flame atomic absorption spectrometry (FAAS), Food Chem. 194 (2016) 373–376. https://doi.org/10.1016/j.foodchem.2015.08.027

[11] G. Cravotto, P. Cintas, Power ultrasound in organic synthesis: moving cavitational chemistry from academia to innovative and large-scale applications, Chem. Soc. Rev. 35 (2006) 180–196. https://doi.org/10.1039/B503848K

[12] K.S. Suslick, G.J. Price, Applications of ultrasound to materials chemistry, Annu. Rev. Mater. Sci. 29 (1999) 295–326. https://doi.org/10.1146/annurev.matsci.29.1.295

[13] K.A. Kusters, S.E. Pratsinis, S.G. Thoma, D.M. Smith, Energy—size reduction laws for ultrasonic fragmentation, Powder Technol. 80 (1994) 253–263. https://doi.org/10.1016/0032-5910(94)02852-4

[14] K.S. Suslick, M.M. Fang, T. Hyeon, M.M. Mdleleni, Applications of sonochemistry to materials synthesis, in: L.A. Crum, T.J. Mason, J.L. Reisse, K.S. Suslick (Eds.), Sonochemistry and Sonoluminescence, Springer, vol 524. Springer, Dordrecht, 524 (1999) pp. 291–320.

[15] T.J. Mason, Some neglected or rejected paths in sonochemistry – a very personal view, Ultrason. Sonochem. 25 (2015) 89–93. https://doi.org/10.1016/j.ultsonch.2014.11.014

[16] N.V. Dezhkunov, T.G. Leighton, Study into correlation between the ultrasonic capillary effect and sonoluminescence, J. Eng. Phys. Thermophys. 77 (2004) 53–61. https://doi.org/10.1023/B:JOEP.0000020719.33924.aa

[17] T.J. Mason, L. Paniwnyk, J.P. Lorimer, The uses of ultrasound in food technology, Ultrason. Sonochem. 3 (1996) S253–S260. https://doi.org/10.1016/S1350-4177(96)00034-X

[18] K. Vilkhu, R. Manasseh, R. Mawson, M. Ashokkumar, Ultrasonic recovery and modification of food ingredients, in: H. Feng, G. Barbosa-Canovas, J. Weiss (Eds.), Ultrasound Technologies for Food and Bioprocessing, Springer, New York, USA, 2011, pp. 345–368. http://link.springer.com/content/pdf/10.1007%2F978-1-4419-7472-3_13

[19] I. Viera, I. Machado, M. Pistón, M.H. Torre, Determination of As, Cd, Cu, Fe, Ni, Pb and Zn in soybean seeds and their correlation with relevant bioinorganic parameters to assess food quality, BrJAC--Braz. J. Anal. Chem. 5 (2018) 26–34.

[20] B. Magnusson, U. Örnemark (Eds.), Eurachem Guide: the Fitness for Purpose of Analytical Methods – A Laboratory Guide to Method Validation and Related Topics, second ed. (2014). ISBN 978-91-87461-59-0. http://www.eurachem.org (accessed February 2019).

[21] K. Mochizuki, N.I. Smith, K. Fujita, Raman Microscopy, Encyclopedia of Analytical Science, third ed., Chemistry, Molecular Sciences and Chemical Engineering (2019) 58–67.

[22] T.H. Kauffmann, M.D. Fontana, Inorganic salts diluted in water probed by Raman spectrometry: Data processing and performance evaluation, Sens. Actuators, B 209 (2015) 154–161. https://doi.org/10.1016/j.snb.2014.11.108

[23] A. Rygula, K. Majzner, K.M. Marzec, A. Kaczor, M. Pilarczyka, M. Baranska, Raman spectroscopy of proteins: a review, J. Raman Spectrosc. 44 (2013) 1061–1076. https://doi.org/10.1002/jrs.4335

[24] F. Elmi, A.F. Movaghar, M.M. Elmi, H. Alinezhad, N. Nikbakhsh, Application of FT-IR spectroscopy on breast cancer serum analysis, Spectrochim. Acta, Part A 187 (2017) 87–91. https://doi.org/10.1016/j.saa

[25] C.B. Brutti, E.J. Rubio, B.E. Llorente, N.M. Apóstolo, Artichoke leaf morphology and surface features in different micropropagation stages, Biol. Plant. 45 (2002) 197–204. https://doi.org/10.1023/A:1015132303698

[26] L. Petigny, S. Périno-Issartier, J. Wajsman, F. Chemat, Batch and continuous ultrasound assisted extraction of boldo leaves (*Peumus boldus* Mol.), Int. J. Mol. Sci. 14 (2013) 5750–5764. https://doi.org/10.3390/ijms14035750

[27] S. Chemat, A. Lagha, H. AitAmar, P.V. Bartels, F. Chemat, Comparison of conventional and ultrasound-assisted extraction of carvone and limonene from caraway seeds, Flavour Fragrance J. 19 (2004) 188–195. https://doi.org/10.1002/ffj.1339

Figure captions

Figure 1 Fragmentation effect of ultrasound. Kinetics of Cu extraction from artichoke leaves (a) and soybean seeds (c) observed for probe- and bath-based UAE, monitored by atomic absorption. Particle size repartition of artichoke leaves (b) and soybean seeds (d) after probe-based UAE.

Figure 2 Raman optical images of the control soybean sample (a), UAE-bath residue (b), and UAE-probe residue (c). (d) Raman spectra of the control soybean sample (black), 10-min UAE-probe residue (red), and 20-min UAE-probe residue (green).

Figure 3 FT-IR spectra of the control soybean sample (blue) and 10-min UAE-probe residue (red).

Figure 4 Erosion effect of ultrasound. SEM images of artichoke leaf surface: control leaves (a), 10-min UAE-probe residue (b) and 20-min UAE-probe residue (20 kHz) (c).

Figure 5 Erosion effect of ultrasound. SEM images of soybean seed surface: control soybean sample (a), 10-min UAE-probe residue (b) and 20-min UAE-probe residue (20 kHz) (c).

Figure 6 Detexturation effect of ultrasound. SEM images of soybean seed surface: 25-min and 30-min UAE-probe residues (b, c).

Table captions

Table 1 Results obtained using MAE, UAE-probe, and UAE-bath procedures.

Table 2 Raman bands observed in the spectra of artichoke samples.

Figure 1

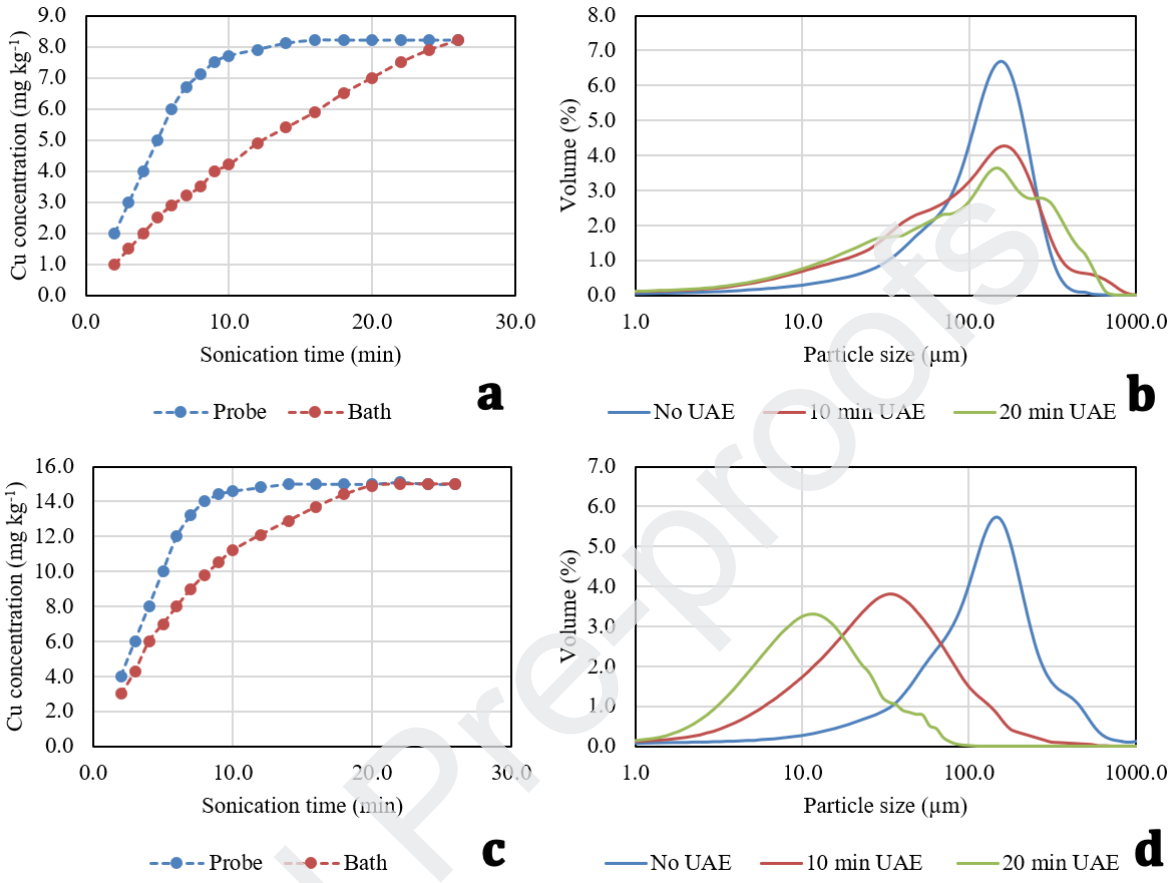

Figure 2

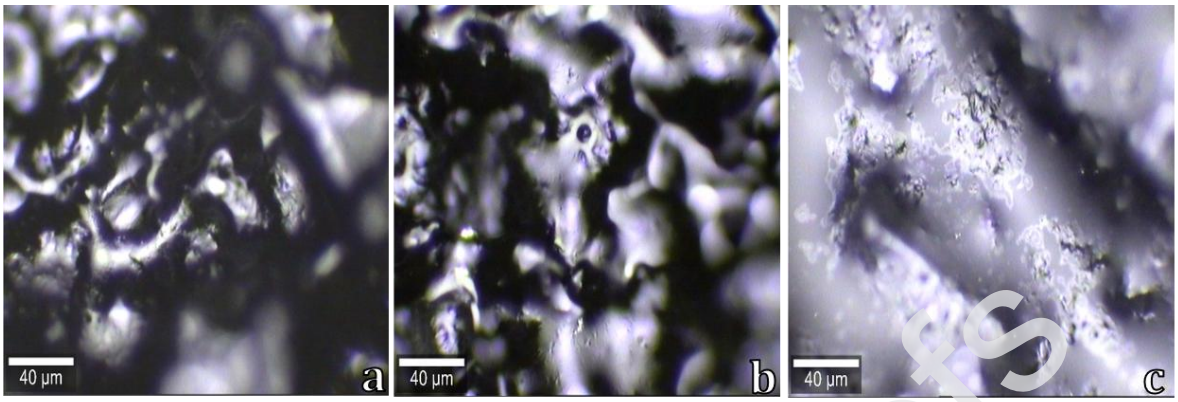

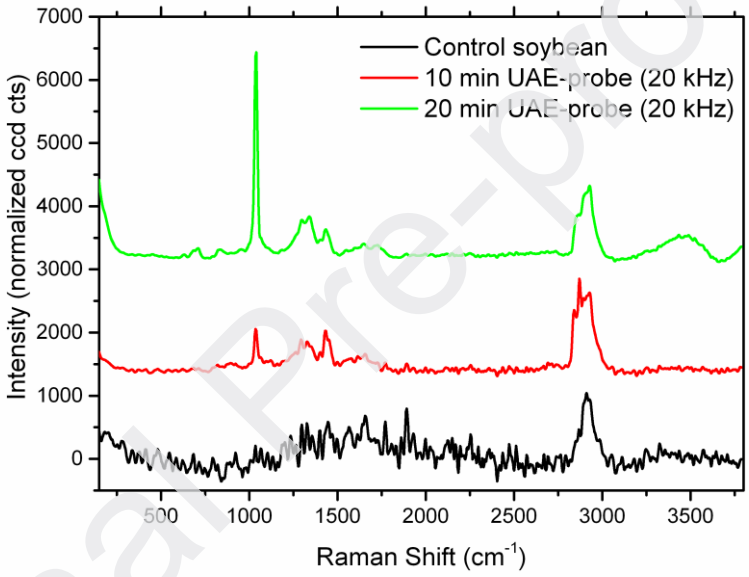

d

Figure 3

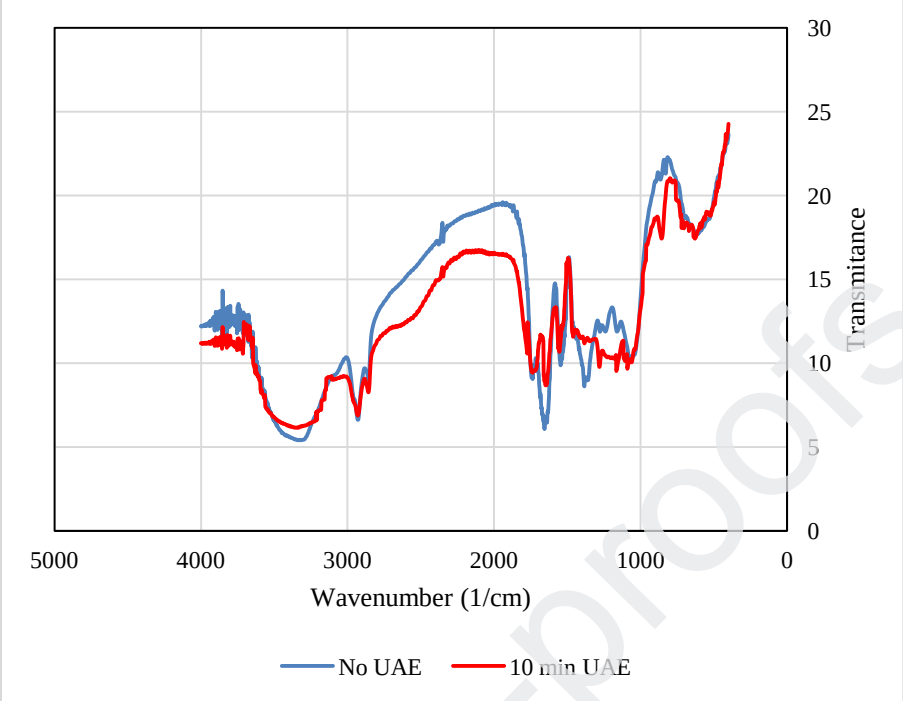

Figure 4

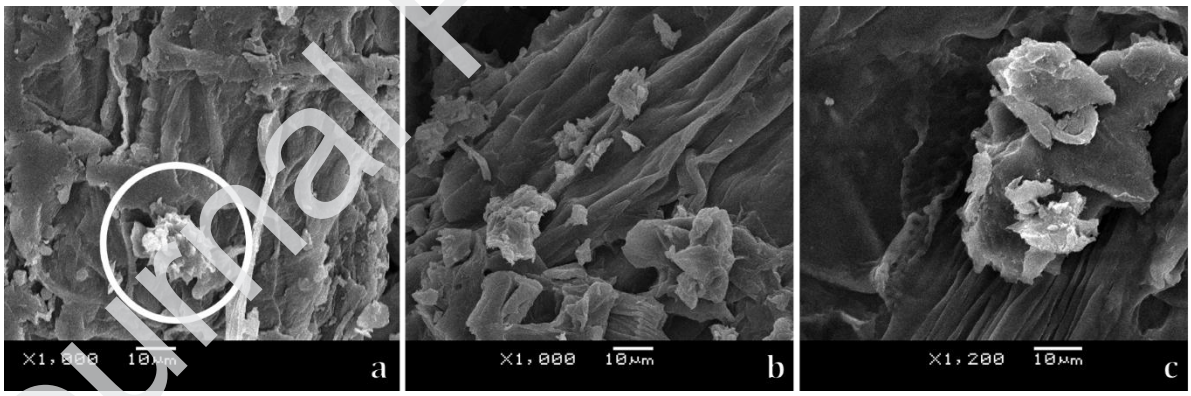

Figure 5

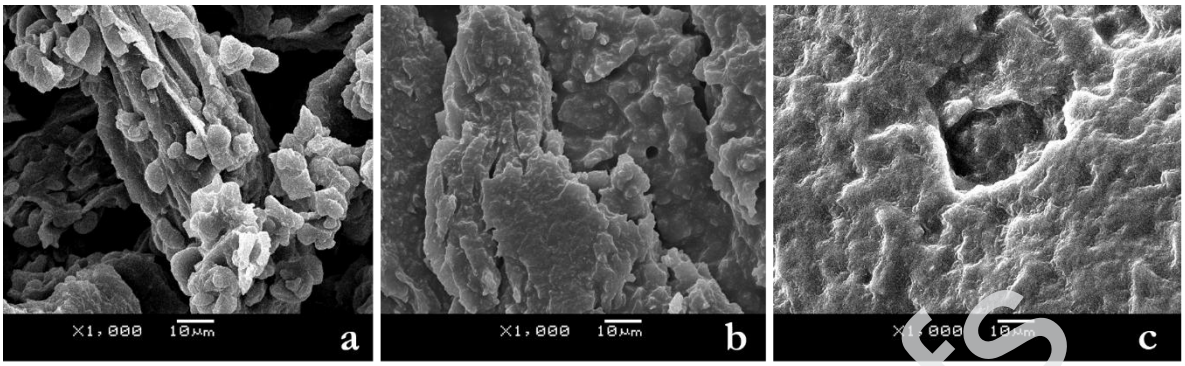

Figure 6

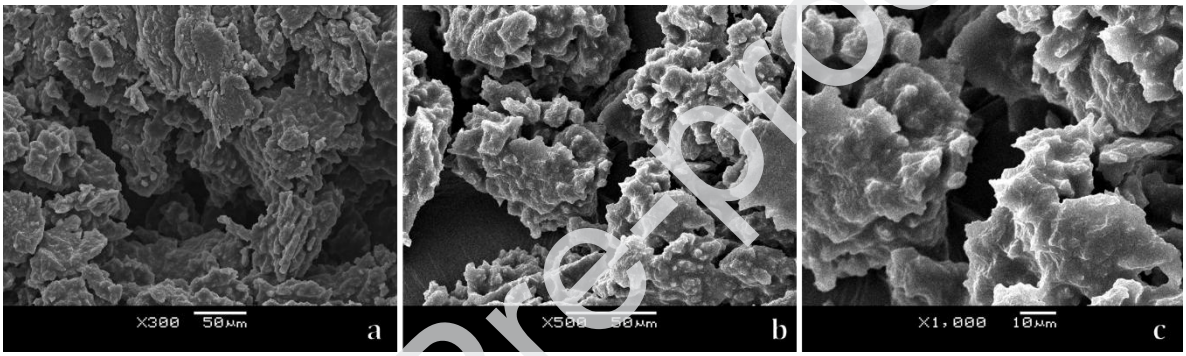

Table 1

Element	Artichoke leaves (mg kg^{-1})			Soybean seeds (mg kg^{-1})		
	MAE	UAE-probe	UAE-bath	MAE	UAE-probe	UAE-bath
Cd	0.19 ± 0.01	0.18 ± 0.02	0.19 ± 0.02	0.013 ± 0.002	0.012 ± 0.002	0.014 ± 0.001
Cu	9.8 ± 0.1	9.3 ± 0.5	9.4 ± 0.3	15.0 ± 0.3	14.3 ± 0.4	14.1 ± 0.5
Ni	1.9 ± 0.2	1.5 ± 0.2	1.5 ± 0.2	9.4 ± 0.1	9.2 ± 0.1	9.0 ± 0.2
Pb	0.32 ± 0.01	0.29 ± 0.01	0.30 ± 0.01	0.112 ± 0.008	0.115 ± 0.007	0.109 ± 0.009
Zn	95.3 ± 0.8	94.2 ± 0.7	95.3 ± 0.4	35.0 ± 0.9	33.2 ± 0.8	31.9 ± 0.9

Mean ± standard deviation (n = 3), dry basis

Table 2

Raman bands (cm^{-1})	Assignment
1038	NO_3^-
1300–1340	$\rho(CH_3)$ + sym $\delta(CH_3)$
1230–1300	Amide II
1430	asym $\delta(CH_3)$
1480–1500	Amide III
1620–1680	Amide I
2931	$\nu(CH_3)$
2800–3000	$\nu(CH_2)$

Highlights

- Ultrasound-assisted extraction of trace elements from model foods was performed
- Fragmentation, erosion and detexturation were characterized
- The developed method complied with Green Chemistry criteria